Structure of Round, Fully Developed, Buoyant Turbulent Plumes

Z. Dai
Graduate Student Research Assistant.

L.-K. Tseng
Research Fellow.

G. M. Faeth
Professor.
Fellow ASME

Department of Aerospace Engineering,
The University of Michigan,
Ann Arbor, MI 48109-2118

An experimental study of the structure of round buoyant turbulent plumes was carried out, emphasizing conditions in the fully developed (self-preserving) portion of the flow. Plume conditions were simulated using dense gas sources (carbon dioxide and sulfur hexafluoride) in a still air environment. Mean and fluctuating mixture fraction properties were measured using single-and two-point laser-induced iodine fluorescence. The present measurements extended farther from the source (up to 151 source diameters) than most earlier measurements (up to 62 source diameters) and indicated that self-preserving turbulent plumes are narrower, with larger mean and fluctuating mixture fractions (when appropriately scaled) near the axis, than previously thought. Other mixture fraction measurements reported include probability density functions, temporal power spectra, radial spatial correlations and temporal and spatial integral scales.

Introduction

Scalar mixing of round buoyant turbulent plumes in a still environment is an important fundamental problem that has attracted significant attention since the classical study of Rouse et al. (1952). However, recent work suggests that more information about the turbulence properties of scalar quantities within buoyant turbulent flows is needed to address turbulence/radiation interactions in fire environments (Kounalakis et al., 1991). In particular, the response of radiation to turbulent fluctuations is affected by the moments, probability density functions, and temporal and spatial correlations of scalar property fluctuations. In turn, scalar property fluctuations can be represented by mixture fraction (defined as the mass fraction of source fluid) fluctuations, using state relationships found from conserved-scalar concepts for both nonreactive and flame environments (Bilger, 1976; Sivathanu and Faeth, 1990). Thus, the objective of the present investigation was to measure mixture fraction statistics in round buoyant turbulent plumes in still environments. In order to simplify interpretation of the results, the experiments emphasized fully developed buoyant turbulent plumes, where effects of the source have been lost and both mean and fluctuating properties become self-preserving (Tennekes and Lumley, 1972).

The discussion of previous studies will be brief because several reviews of turbulent plumes have appeared recently (Kotsovinos, 1985; List, 1982; Papanicolaou and List, 1987, 1988). The earliest work concentrated on the scaling of flow properties within fully developed turbulent plumes (Rouse et al., 1952; Morton, 1959; Morton et al., 1956). Measurements of mean properties within plumes generally have satisfied the resulting scaling relationships; however, there are considerable differences among various determinations of centerline values, radial profiles, and flow widths (Abraham, 1960; George et al., 1977; Kotsovinos, 1985; List, 1982; Ogino et al., 1980; Peterson and Bayazitoglu, 1992; Shabbir and George, 1992; Rouse et al., 1952; Zimin and Frik, 1977). Aside from problems of experimental methods in some instances, List (1982) and Papanicolaou and List (1987, 1988) attribute these differences to problems of reaching fully developed plume conditions.

Two parameters are helpful for estimating when turbulent plumes become self-preserving. The first of these is the distance from the virtual origin normalized by the source diameter, $(x-x_o)/d$. Based on results for nonbuoyant round turbulent jets, values of $(x-x_o)/d$ greater than ca. 40 and 100 should be required for self-preserving profiles of mean and fluctuating properties, respectively (Tennekes and Lumley, 1972). By these measures, all past measurements over the cross section of plumes, which invariably used buoyant jets for the plume source, probably involve transitional plumes, e.g., they generally are limited to $(x-x_o)/d \leq 62$, aside from some limited measurements in liquids by Papantoniou and List (1989). The main reason for not reaching large values of $(x-x_o)/d$ for plumes, similar to jets, is that scalar properties decay much faster for plumes, e.g., proportional to $(x-x_o)^{-5/3}$ for plumes rather than $(x-x_o)^{-1}$ for jets. Thus, it is difficult to maintain reasonable experimental accuracy far from the source within the plumes. A contributing factor is that plume velocities are relatively small in comparison to jets so that controlling room disturbances far from the source is more difficult for plumes.

The second parameter useful for assessing conditions for self-preserving buoyant turbulent plumes is the distance from the virtual origin normalized by the Morton length scale, $(x-x_o)/l_M$. The Morton length scale is defined as follows for a round plume having uniform properties at the source (Morton, 1959; List, 1982):

$$l_M = (\pi/4)^{1/4}(\rho_\infty d u_o^2/(g|\rho_o - \rho_\infty|))^{1/2} \quad (1)$$

where an absolute value has been used for the density difference in order to account for both rising and falling plumes. Large values of $(x-x_o)/l_M$ are required for buoyancy-induced momentum to become large in comparison to the source momentum so that the buoyant features of the flow are dominant. The ratio of l_M to d is proportional to the source Froude number, defined as follows (List, 1982):

$$\mathrm{Fr}_o = (4/\pi)^{1/4} l_M/d = (\rho_\infty u_o^2/(g|\rho_o - \rho_\infty|d))^{1/2} \quad (2)$$

The source Froude number quantifies the initial degree of buoyant behavior of the source, e.g., $\mathrm{Fr}_o = 0$ for a purely buoyant source. Papanicolaou and List (1987, 1988) suggest that buoyancy-dominated conditions for mean and fluctuating quantities are reached for $(x-x_o)/l_M$ greater than ca. 6 and 14, respectively. A greater proportion of existing data for mean properties exceed this criterion; however, the effect of transitional plume behavior (in terms of $(x-x_o)/d$) on these observations raises questions about the adequacy of this criterion.

Naturally, in instances where reaching self-preserving con-

Contributed by the Heat Transfer Division and presented at the National Heat Transfer Conference, Georgia, August 8-11, 1993. Manuscript received by the Heat Transfer Division March 1993; revision received July 1993. Keywords: Fire/Flames, Natural Convection, Turbulence. Associate Technical Editor: Y. Jaluria.

ditions for mean properties is questionable, it is likely that turbulent properties are transitional. Thus, the turbulence measurements of George et al. (1977) and Shabbir and George (1992) for x/d in the range 8–25, normally would not be thought to represent self-preserving conditions. The turbulence measurements of Papanicolaou and List (1987, 1988) for x/d in the range 12–62 probably represent transitional plumes as well with results at larger distances, x/d, of 20–62, subject to additional uncertainties due to systematic instrument errors (Papanicolaou and List, 1988). In contrast, the measurements of Papantoniou and List (1989) were carried out at $x/d = 105$, which should be within the self-preserving region; however, unusually large concentation fluctuations were observed, which they attribute to the large Schmidt numbers of the liquid plumes used in these tests, i.e., molecular mixing was inhibited at small scales that still could be resolved by their instrument system. Thus, the relevance of the Papantoniou and List (1988) turbulence measurements to gaseous plumes of interest for radiation processes in flame environments is questionable.

The preceding discussion suggests that existing measurements of mean and fluctuating properties within plumes probably involve either transitional plumes or liquid plumes exhibiting large Schmidt number effects that are not typical of gases. Thus, the objective of the present investigation was to complete measurements of the mean and fluctuating mixture fraction properties of buoyant turbulent plumes in gases, emphasizing conditions within the self-preserving turbulent plume region where the specific features of the source have been lost. The mixture fraction properties considered included mean and fluctuating values, probability density functions, temporal power spectra, radial spatial correlations, and temporal and spatial integral scales. The experiments involved source flows of carbon dioxide and sulfur hexafluoride in still air at atmospheric pressure and temperature, in order to provide a straightforward specification of the buoyancy flux within the test plumes. This approach yielded downward-flowing, negatively buoyant plumes. Measurements of mixture fraction properties were undertaken using laser-induced iodine fluorescene (LIF).

Experimental Methods

Test Apparatus. A sketch of the experimental apparatus is shown in Fig. 1. In order to minimize room disturbances and contamination of adjacent areas by iodine vapor, the plumes were observed in a double enclosure contained within a large, high-bay test area. The outer enclosure ($3000 \times 3000 \times 3400$ mm high) had plastic side walls with a screen across the top for air inflow in order to compensate for removal of air entrained by the plume. The plume itself was within a smaller enclosure ($1100 \times 1100 \times 3200$ mm high) with plastic screen walls (square pattern, 630 wires/m with a wire diameter of 0.25 mm). The small enclosure was mounted on linear bearings and could be traversed in one direction using a stepping motor driven linear positioner (5 μm positioning accuracy) in order to accommodate rigidly mounted instrumentation. The plume flow was removed through 300-mm-dia ducts that were mounted on the floor at the four corners of the outer enclosure. The exhaust flow was controlled by a bypass/damper system in order to match plume entrainment rates and to minimize flow disturbances. All components that might contact iodine vapor were plastic, painted, or sealed in plastic wrap, in order to prevent corrosion.

The plume sources consisted of rigid plastic tubes having inside diameters of 6.4 and 9.7 mm with flow straighteners at

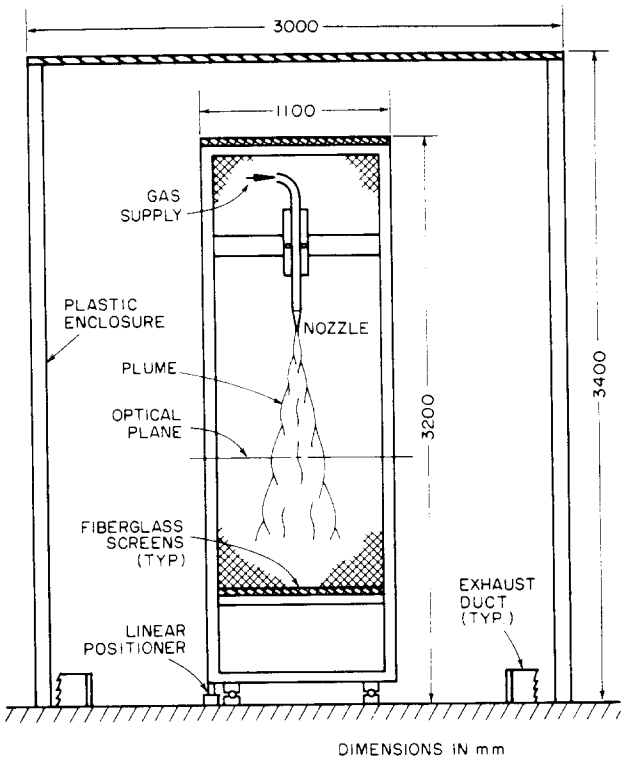

Fig. 1 Sketch of the buoyant turbulent plume apparatus

Nomenclature

a, b = parameters in the Frenkiel function
d = source diameter
$E_f(n)$ = temporal power spectral density of f
f = mixture fraction
$F(r/(x-x_o))$ = scaled radial distribution of $\bar{f}$ in self-preserving region
Fr_o = source Froude number, Eq. (2)
g = acceleration of gravity
k_f = plume width coefficient, Eq. (8)
l_c = characteristic plume radius
l_f = characteristic plume radius based on mean mixture fraction
l_M = Morton length scale, Eq. (1)
n = frequency
PDF(f) = probability density function of mixture fraction
r = radial distance
Re_c = characteristic plume Reynolds number $= \bar{u}_c l_c / \nu_\infty$
Re_o = source Reynolds number $= u_o d / \nu_o$
u = streamwise velocity
x = streamwise distance
Δr = radial distance increment
Λ_{fr} = radial spatial integral scale of mixture fraction fluctuations
ν = kinematic viscosity
ρ = density
τ_f = temporal integral scale of mixture fraction fluctuations

Subscripts

c = centerline value
o = initial value or virtual origin location
∞ = ambient value

Superscripts

$(\bar{\ })$ = time-averaged mean value
$(\bar{\ })'$ = root-mean-squared fluctuating value

the inlet and length-to-diameter ratios of 50:1. The outside surface of the tubing exit was chamfered at an angle of 30 deg to reduce the separation disturbances of the plume-entrained flow. The source could be traversed in the vertical direction (0.25 mm positioning accuracy) to allow measurements at different streamwise positions. The source flows were either carbon dioxide or sulfur hexafluoride, stored under pressure in commercial cylinders. Gas flow rates were controlled and measured using pressure regulators in conjunction with critical flow orifices. All flow rates were calibrated using wet test meters. After metering and adding iodine vapor, the flow passed through a flexible plastic tube having a length-to-diameter ratio of 800 in order to obtain a uniform composition at the source exit.

The flow was seeded with iodine vapor by passing a portion of it though a bed of iodine crystals (bed diameter and depth of 100×200 mm). The bed operated at room temperature and the flow was saturated with iodine at the exit of the bed; therefore, the concentration of iodine vapor varied with changes of room temperature. Thus, the LIF signal was monitored with the fraction of flow entering the iodine bed periodically adjusted to control signal levels. The iodine crystals were reagent grade, with initial flake shapes having diameters of 2–8 mm and thicknesses of 0.5 mm.

Instrumentation. Mixture fractions were measured using LIF, similar to earlier studies of wall plumes in this laboratory (Lai and Faeth, 1987). The LIF signal was produced by the unfocused beam (beam diameter at the e^{-2} points of 1.5 mm) of an argon-ion laser having an optical power of roughly 1800 mW at the green (514.5 nm) line. This wavelength is absorbed by iodine and causes it to fluoresce at longer wavelengths in the visible yellow portion of the spectrum (Hiller and Hanson, 1990). The laser beam was horizontal and intersected the plume axis at roughly 1500 mm above the floor of the enclosure. The operation of the laser beam was monitored using two laser power meters: one measuring laser power before crossing the flow to detect laser power variations, the other measuring laser power after passing through the flow in order to correct the laser beam power at the measuring locations for absorption by iodine vapor.

The fluorescence signals were measured using two detectors (Hamamatsu R269), one mounted rigidly and the other traversable along the laser beam to provide measurements of two-point spatial correlations. Since the plume source could be traversed horizontally and vertically, all points in the flow could be addressed for two-point measurements. The fluorescence signals were observed at right angles to the laser beam with f4.1 collecting lenses having diameters of 80 mm. The apertures of the detectors were selected to give measuring volumes having diameters of 1 mm with lengths of 1.5 mm set by the laser beam diameter. The LIF signal was separated from light scattered at the laser line using long-pass optical filters (cut-off wavelengths of 520 nm). The detector outputs were amplified and then low-pass filtered to control alias signals using sixth-order Chebychev filters having break frequencies of 500 Hz. The signals were then sampled using an a/d converter and transferred to a computer for processing and storage. The detector signals were monitored using a digital oscilloscope as well.

Both the absorption and the LIF signals were calibrated based on measurements across the source exit, by mixing the source flow with air to vary the mixture fraction. These tests showed that fluctuations of iodine seeding levels were less than 1 percent. The LIF signal was not saturated for present conditions and varied linearly with laser power. The LIF signals also varied linearly with the number of iodine molecules present per unit volume (i.e., with the partial density of iodine) while reabsorption of scattered light was small (less than 10 percent). Thus, the relationship between the LIF signal level and the mixture fraction for signal processing was obtained from the state relationship for an ideal gas mixture. This relationship was nearly linear for the carbon dioxide source flow due to modest density variations but had significant nonlinearities for the sulfur hexafluoride source flow where the density variation was substantial. These calibrations were checked periodically by diverting the source flow through a plastic tube whose exit was mounted temporarily just above the measurement location. Final processing of the signals accounted for both absorption of the laser beam by iodine vapor and laser beam power variations.

Table 1 Summary of test conditions[a]

Source Properties	CO_2	SF_6
Density (kg/m^3)	1.75	5.87
Kinematic viscosity (mm^2/s)	8.5	2.6
Diameter (mm)	9.7	6.4
Average velocity (m/s)	1.74	1.89
Reynolds number	2000	4600
Froude number	7.80	3.75
Morton length scale, ℓ_M/d	7.34	3.53
Virtual origin, x_o/d	12.7	0.0

[a]Flow directed vertically downward in still air with an ambient pressure, temperature, density and kinematic viscosity of 99 ± 0.5 kPa, 297 ± 0.5 K, 1.16 kg/m^3 and 14.8 mm^2/s. Source passage length-to-diameter ratios of 50:1.

Differential diffusion between the source gas (carbon dioxide or sulfur hexafluoride) and the iodine vapor can be a significant source of error for LIF measurements. Effects of differential diffusion were evaluated analogous to the approach described by Stårner and Bilger (1983), noting that the binary diffusivities of carbon dioxide, sulfur hexafluoride, and iodine in air at normal temperature and pressure are 14.7, 8.6, and 7.7 mm^2/s (Bird et al., 1960). This yielded maximum errors of mean mixture fractions due to differential diffusion for the carbon dioxide and sulfur hexafluoride plumes less than 2 and 0.2 percent, respectively, with comparable values for mixture fraction fluctuations. The present measurements corroborated these results, based on the observation that the source gas had little effect on mixture fraction properties in the self-preserving region of the flow.

Gradient broadening errors were negligible (less than 1 percent) at the locations where measurements were made. Thus, signal sampling times were controlled to maintain experimental uncertainties (95 percent confidence) along the axis at less than 5 percent for mean mixture fractions and 10 percent for mixture fraction fluctuations, both being repeatable well within these ranges. These uncertainties were maintained up to $r/(x-x_o) = 0.15$ but increased at larger radial distances, roughly inversely proportional to $\bar{f}$.

Test Conditions. The test conditions for the carbon dioxide and sulfur hexafluoride plumes are summarized in Table 1. An attempt was made to keep source Froude numbers near current estimates of asymptotic Froude numbers in order to enhanced the development of the buoyancy properties of the flow (George et al., 1977). Additionally, source Reynolds numbers were made as large as possible, while satisfying the Froude number requirement, in order to enhance rates of development toward self-preserving turbulent plume conditions. Nevertheless, the Reynolds number of the carbon dioxide flow was relatively low, 2000, causing the virtual origin to be displaced a substantial distance downstream from the source exit. For $(x-x_o)/d$ greater than 87, where self-preserving plumes were reached, the turbulence microscales of mixture fraction fluctuations (the Batchelor scales) were less than 350 μm. Thus, although the previously stated experimental uncertainties were achieved, the spatial resolution of the LIF system was not

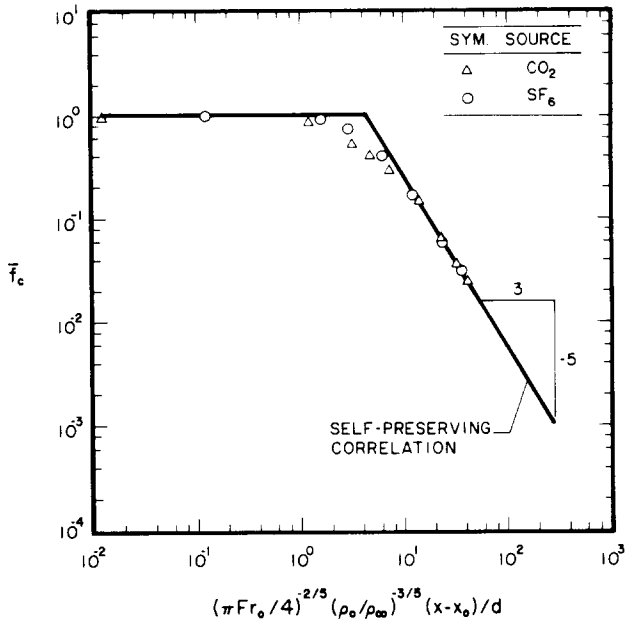

Fig. 2 Mean mixture fractions along the axis

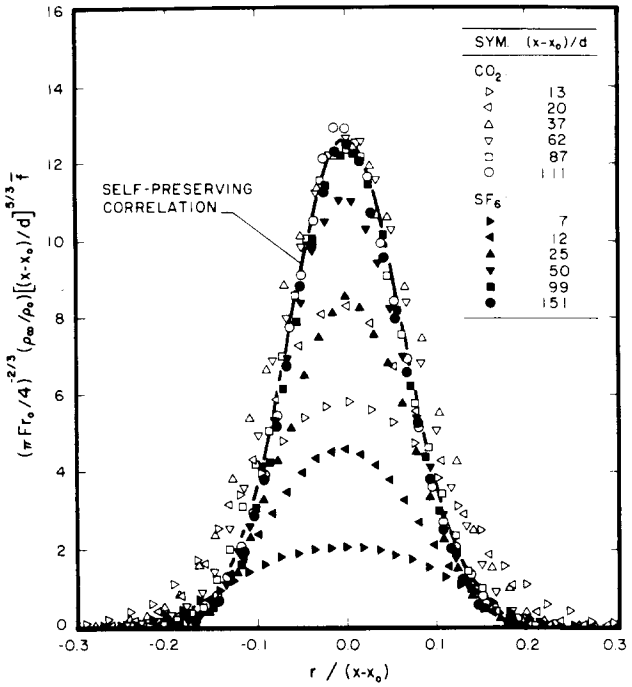

Fig. 3 Development of radial profiles of mean mixture fractions

sufficient to resolve the smallest scales of the turbulence within the self-preserving region of the plumes.

Self-Preserving Scaling

The state relationship for density as a function of mixture fraction is needed to relate the present measurements to properties in the self-preserving region. Assuming an ideal gas mixture, the exact state relationship for density becomes:

$$\rho = \rho_\infty/(1 - f(1 - \rho_\infty/\rho_o)) \tag{3}$$

Additionally, far from the source in the self-preserving region, $f \ll 1$, and Eq. (3) can be linearized as follows:

$$\rho = \rho_\infty + f\rho_\infty(1 - \rho_\infty/\rho_o), \qquad f \ll 1 \tag{4}$$

The measurements involved mean and fluctuating mixture fraction properties at various streamwise positions. Mean properties were then scaled in terms of the self-preserving variables of fully developed turbulent plumes, as follows (List, 1982):

$$\bar{f} = (\pi \mathrm{Fr}_o/4)^{2/3}(\rho_o/\rho_\infty)((x-x_o)/d)^{-5/3}F(r/(x-x_o)) \tag{5}$$

$F(r/x-x_o))$ represents the appropriately scaled radial profile function of mean mixture fraction, which becomes a universal function in the self-preserving region far from the source where Eq. (4) applies. Equation (5) was used to extrapolate measurements of mean mixture fractions along the axis in order to identify the virtual origin that yielded the best fit of the data. As noted earlier, the location of the virtual origin is controlled by source properties like turbulence levels, ρ_o/ρ_∞, and the initial Froude numbers; however, it was beyond the scope of the present investigation to quantitatively study these relationships.

Finally, although velocity measurements were not made during the present study, it was of interest to find characteristic plume Reynolds numbers, $\mathrm{Re}_c = \bar{u}_c l_c/\nu_\infty$. This was done by adopting the expressions of Rouse et al. (1952) for $\bar{u}_c$ and l_c at self-preserving conditions to yield:

$$\mathrm{Re}_c = 0.43((x-x_o)/(d\,\mathrm{Fr}_o))^{2/3}u_o d/\nu_\infty \tag{6}$$

Results and Discussion

Mean Properties. The variation of mean mixture fractions along the axis of the two test plumes is illustrated in Fig. 2. The measurements are plotted in terms of the variables of Eq. (5). In addition, lines showing the asymptotic behavior of the present measurements at small and at large distances from the source are shown on the plot. The limiting behavior at small distances , $(x-x_o)/d \ll 1$, is $\bar{f}_c = 1$ which the measurements satisfy by definition. The limit at large distances follows from Eq. (5) for conditions where $\bar{f}_c \ll 1$ and Eq. (4) applies. Then $F(0) = 12.6$ independent of source flow properties, based on the best fit of present measurements, and $\bar{f}_c \sim ((x-x_o)/d)^{-5/3}$. This latter condition is reached for values of the abscissa of Fig. 2 greater than 10, which implies $(x-x_o)/d$ and $(x-x_o)/l_M$ on the order of 100 and 10, respectively. Within the intermediate region, where the abscissa of Fig. 2 is in the range 0.1-10, results depend on source properties like Re_o, Fr_o, and ρ_o/ρ_∞ so that the differences in this region seen in Fig. 2 for the two sources are anticipated. Naturally, this implies that conditions required to reach self-preserving plume behavior depend on these variables as well.

A more complete picture of the development of transitional plumes toward self-preserving conditions can be obtained from the radial profiles of mean mixture fractions for the two sources illustrated in Fig. 3. In this case, the scaling parameters of Eq. (5) are used so that the ordinate is equal to $F(r/x-x_o))$. The measurements are plotted for various streamwise distances with $(x-x_o)/d \geq 7$. The radial mean mixture fraction profiles show progressive narrowing, with scaled values at the axis progressively increasing, as the streamwise distance increases. However, self-preserving conditions are observed for the present measurements when $(x-x_o)/d \geq 87$, which also corresponds to $(x-x_o)/l_M \geq 12$. The subsequent variation of the profiles with streamwise distance is well within experimental uncertainties over the range that was achieved during the present experiments: $87 \leq (x-x_o)/d \leq 151$ and $12 \leq (x-x_o)/l_M \leq 43$. This regime corresponds to characteristic plume Reynolds numbers of 2500–4200, which are reasonably high for unconfined turbulent flows. For example, this range is comparable to the highest characteristic wake Reynolds numbers where measurements of turbulent wake properties have been reported, while turbulent wakes exhibit self-preserving turbulence properties at characteristic wake Reynolds numbers as low as 70 (Wu and Faeth, 1993). The actual streamwise distance required

Table 2 Summary of self-preserving turbulent plume properties[a]

Source	Medium	$(x-x_o)/d$	$(x-x_o)/\ell_M$	k_f^2	$\ell_f/(x-x_o)$	$F(0)$	$(\bar{f}'/\bar{f})_c$
Present study	gaseous	87-151	12-43	125	0.09	12.6	0.45
Papantoniou and List (1989)	liquid	105	24,33	---	0.08-0.09	---	0.64
Papanicolaou and List (1988)	liquid	22-62	9-62	80	0.11	14.3	0.40
Papanicolaou and List (1987)	liquid	12-20	> 5	80	0.11	11.1	0.40
Shabbir and George (1992)	gaseous	10-25	6-15	68	0.12	9.4	0.40
George et al. (1977)	gaseous	8-16	6-12	65	0.12	9.1	0.40

[a]Round turbulent plumes in still, unstratified environments. Range of streamwise distances are for conditions where quoted self-preserving properties were found from measurements over the cross section of the plumes. Entries are ordered in terms of decreasing k_f.

to reach self-preserving conditions for mean mixture fractions, however, is likely to vary with source properties. For example, larger values of ρ_o/ρ_∞ and lower source Reynolds numbers tend to retard development toward self-preserving conditions, based on present findings during preliminary tests, while larger source Froude numbers require larger values of $(x-x_o)/d$ in order to achieve values of $(x-x_o)/l_M$ where buoyancy dominates flow properties.

Within the self-preserving region, present radial profiles of mean mixture fractions are reasonably approximated by a Gaussian fit, similar to past work (Rouse et al., 1952; George et al., 1977; List, 1982; Papanicolaou and List, 1987, 1988; Shabbir and George, 1992) as follows:

$$F(r/(x-x_o)) = F(0)\exp\{-k_f^2(r/(x-x_o))^2\} \quad (7)$$

where

$$k_f = (x-x_o)/l_f \quad (8)$$

Thus, l_f represents the characteristic plume radius where $\bar{f}/\bar{f}_c = e^{-1}$. The best fit of the present data in the self-preserving region yielded $F(0) = 12.6$ and $k_f^2 = 125$. This yielded the correlation illustrated in Fig. 3, which is seen to be a good representation of the measurements in the self-preserving region, i.e., $(x-x_o)/d \geq 87$ and $(x-x_o)/l_M \geq 12$. This yields a value of $l_f/(x-x_o)$ of roughly 0.09, which is in good agreement with the values of 0.08–0.09 found by Papantoniou and List (1989) for measurements at large distances from the source, $(x-x_o)/d = 105$ and $(x-x_o)/l_M$ of 24 and 33.

The present values of normalized streamwise distance required to reach self-preserving conditions within round buoyant turbulent plumes are similar to past observations for round turbulent jets (Hinze, 1975; Tennekes and Lumley, 1972); however, they are substantially larger than streamwise distances reached during past measurements of the self-preserving properties of turbulent plumes using buoyant jet sources, aside from the study of Papantoniou and List (1989). This behavior is quantified in Table 2, where the range of streamwise distances considered for measurements of radial profiles of self-preserving plume properties, and the corresponding reported values of k_f^2, $l_f/(x-x_o)$, and $F(0)$ are summarized for representative recent studies and associated earlier work from the same laboratories. Past measurements generally satisfy the criterion for buoyancy-dominated flow, i.e., $(x-x_o)/l_M > 6$ (Papanicolaou and List, 1987, 1988). Aside from the measurements of Papantoniou and List (1989) and the present study, however, the other results were obtained at values of $(x-x_o)/d$ that normally are not associated with self-preserving conditions for jetlike sources. Somewhat like the tendency for transitional plume conditions to have broader profiles than the self-preserving regime in Fig. 3, the values of k_f^2 tend to increase progressively as the maximum streamwise position is increased—almost doubling over the range of conditions given in Table 2. This yields a corresponding reduction of characteristic plume radius of 30 percent, and an increase of the scaled mean mixture fraction at the axis of 30 percent, when approaching self-preserving conditions over the range considered in Table 2 (ignoring the unusually large value of $F(0)$ reported by Papanicolaou and List (1988), which is thought to be due to a systematic instrument error, as noted earlier). Discrepancies between transitional and self-preserving plumes of this magnitude have a considerable impact on the empirical parameters obtained by fitting turbulence models to measurements. For example, Pivovarov et al. (1992) suggest that the standard set of constants used in empirical turbulence models is inadequate based on the assumption of self-preserving plumes in conjunction with past measurements for transitional plumes; however, their predictions using standard constants are in fair agreement with the present measurements of self-preserving plume properties under the same assumptions.

Root-Mean-Square Fluctuations. Radial profiles of mixture fraction fluctuations at various streamwise distances are plotted in Fig. 4 for the two sources. Near the source, the profiles are rather broad and exhibit a dip as the axis is approached, much like the behavior of nonbuoyant jets (Becker et al., 1967; Papanicolaou and List, 1987, 1988). The profiles evolve, however, with both the width and the magnitude of the dip near the axis gradually decreasing as the streamwise distance is increased. Eventually, self-preserving behavior is reached at conditions similar to the self-preserving conditions for mean mixture fractions in Fig. 3, e.g., $(x-x_o)/d \geq 87$ and $(x-x_o)/l_M \geq 12$. This behavior is not surprising because self-preserving conditions for mean properties are a generally necessary condition for self-preserving conditions for turbulence properties (Tennekes and Lumley, 1972). Within the self-preserving region, present measurements can be correlated reasonably well by the following empirical relationship:

$$\bar{f}'/\bar{f}_c = 0.45\ \exp(-40(r/(x-x_o))^{2.5}) \quad (9)$$

Analogous to mean mixture fractions, the measurements of rms mixture fraction fluctuations of Papanicolaou and List (1987, 1988), Shabbir and George (1992), and George et al. (1977) are similar to transitional plumes in the latter stages of development. Thus, although these profiles do not exhibit a dip near the axis, they are broader in terms of $r/(x-x_o)$ than the present measurements in the self-preserving region. Additionally, Papanicolaou and List (1987, 1988), Shabbir and George (1992), and George et al. (1977) find $(\bar{f}'/\bar{f})_c = 0.40$, rather than 0.45 for the present measurements, as summarized in Table 2. On the other hand, Papantoniou and List (1989) measure $(\bar{f}'/\bar{f})_c$ of roughly 0.64 at conditions that should be within the self-preserving region; however, as discussed earlier, this large value probably is caused by the large Schmidt number of their liquid plumes, which inhibits small-scale mixing in comparison to plumes in gases.

The gradual disappearance of the dip in mixture fraction fluctuations is an interesting feature of the results illustrated

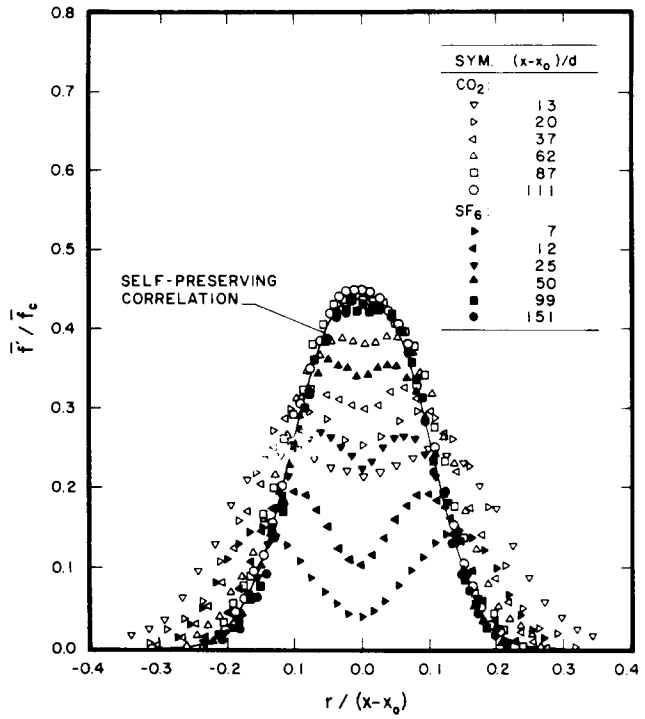

Fig. 4 Development of radial profiles of rms mixture fraction fluctuations

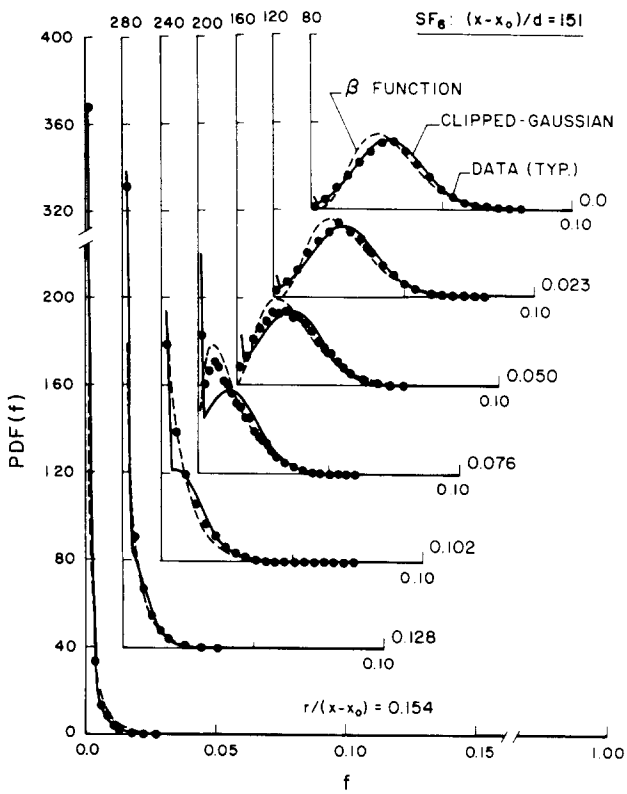

Fig. 5 Typical probability density functions of mixture fractions at self-preserving conditions: SF$_6$ soruce at $(x-x_o)/d$ = 151

in Fig. 4. The development of the flow from source conditions, where mixture fraction fluctuations are less than 1 percent, is certainly a factor in this behavior. However, the gradual disappearance of nonbuoyant dynamics as $(x-x_o)/l_M$ becomes large also is a factor. In particular, nonbuoyant jets have reduced mixture fraction fluctuations near the axis because turbulence production is small in this region in view of symmetry requirements (Becker et al., 1967; Papanicolaou and List, 1987, 1988). In contrast, effects of buoyancy provide turbulence production near the axis for plumes in spite of symmetry due to buoyant instability in the streamwise direction, i.e., the density approaches the ambient density in the streamwise direction. This added turbulence production accounts for increased mixture fraction fluctuation levels near the axis of plumes in comparison to jets in the self-preserving region, i.e., $(\bar{f}'/\bar{f})_c$ ca. 0.45 for plumes in comparsion to 0.15–0.18 for jets (Papanicolaou and List, 1987). Even maximum values of $\bar{f}'/\bar{f}_c$ in jets, ca. 0.25 at an $r/(x-x_o)$ of roughly 0.1, are substantially less than the maximum plume values (Papanicolaou and List, 1987). Thus, the contribution of buoyancy to turbulence is appreciable, with the large mixture fraction fluctuations of turbulent self-preserving plumes helping to explain the large radiation fluctuation levels observed in the plumes above buoyant turbulent diffusion flames (Kounalakis et al., 1991).

Probability Density Functions. Mean and fluctuating velocities are reasonably descriptive because the probability density functions of velocities in turbulent flows generally are well represented by a Gaussian distribution function that only has two moments. This is not the case for the probability density functions of mixture fracture, however, because the mixture fraction is limited to the finite range 0–1 by definition, so that finite range distribution functions must be used, e.g., the clipped-Gaussian function or the algebraically more convenient beta function; see Lockwood and Naguib (1975) for the properties of these two distributions. Thus, some typical probability density functions from present measurements are plotted along with these distribution in Fig. 5. Both distributions are defined by two moments; thus, the predicated distributions are based on the measured values of $\bar{f}$ and $\bar{f}'$ at each location considered.

The measured probability density functions illustrated in Fig. 5 are qualitatively similar to earlier measurements for flames, plumes, and jets (Kounalakis et al., 1991; Papanicolaou and List, 1987, 1988; Becker et al., 1967). At the axis, the probability density function is nearly Gaussian, although it still has a small spike at $f = 0$ representing some period when unmixed ambient fluid reaches the axis. With increasing radial distance, the spike at $f = 0$ increases and eventually dominates the distribution as the edge of the plume is approached. There is little to choose between representing the probability density functions by either clipped-Gaussian or beta functions although the ease of use of the beta function is helpful for reducing computation times during simulations (Lockwood and Naguib, 1975).

Temporal Power Spectral Densities. Temporal correlations, or temporal power spectral densities, which are their Fourier transform (Hinze, 1975; Tennekes and Lumley, 1972), must be known in order to simulate the temporal aspects of radiation fluctuations (Kounalakis et al., 1991). Some typical measurements of temporal power spectra for the sulfur hexafluoride plumes are illustrated in Fig. 6; results for the carbon dioxide plumes were similar. Spectra are plotted for $(x-x_o)/d$ in the range 25–151, considering radial positions over the full width of the flow at each streamwise position. The temporal spectra are relatively independent of radial position at at particular streamwise location. Similarly, the low-frequency portion of the spectra is relatively independent of streamwise distance when normalized in the manner of Fig. 6. However, there are systematic variations in the decaying portion of the spectra with streamwise distance that will be discussed next. Spectra of transitional plumes reported by Papanicolaou and List (1987, 1988) are qualitatively quite similar to the results illustrated in Fig. 6.

The decay of the spectra with increasing frequency is an interesting feature of the results illustrated in Fig. 6. The spectra initially decay according to the $-5/3$ power of frequency.

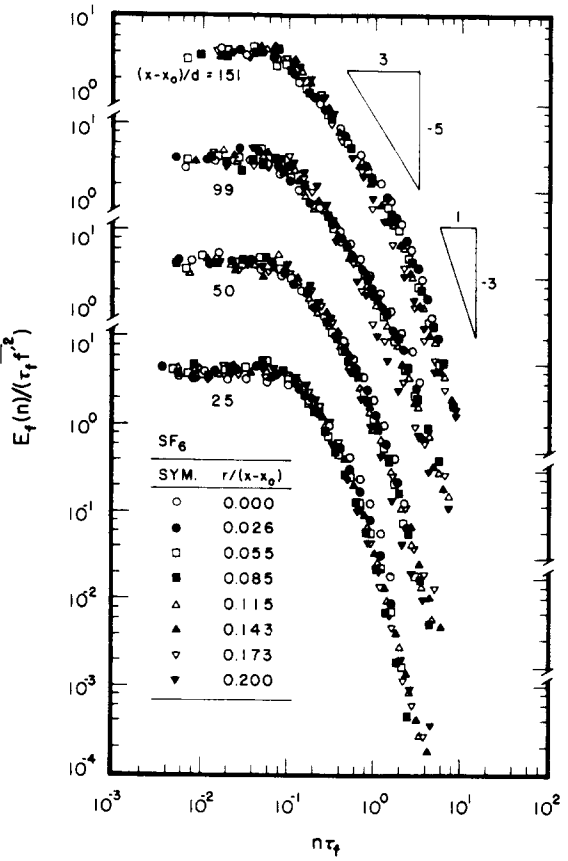

Fig. 6 Typical temporal power spectral densities of mixture fraction fluctuations: SF_6 source

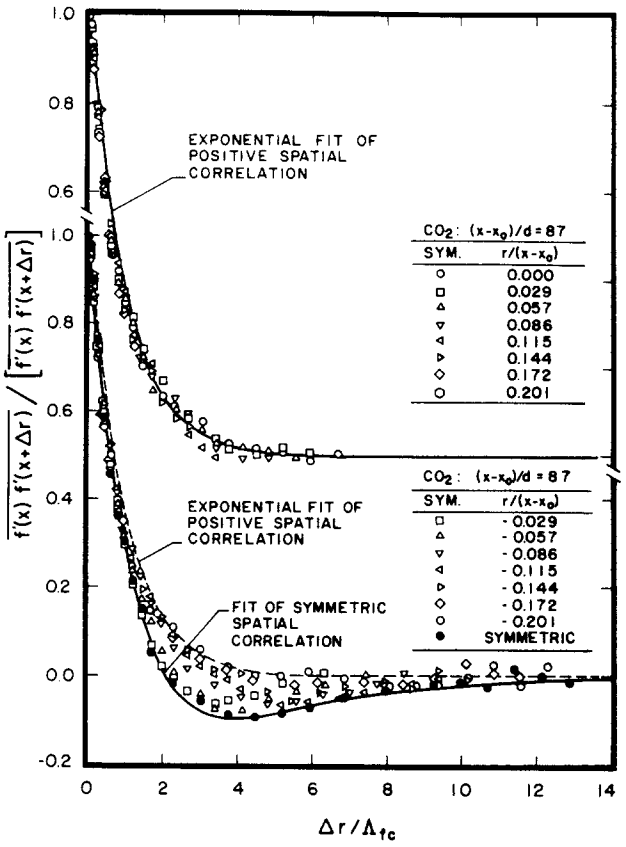

Fig. 7 Typical radial spatial correlations of mixture fraction fluctuations: CO_2 source

analogous to the well-known inertial region of the turbulence spectrum of velocity fluctuations which has been called the intertial-convective region for scalar property fluctuations (Tennekes and Lumley, 1972). Within this region, mixture fraction fluctuations simply are convected and effects of molecular diffusitivies are small. This is followed by a region where the spectrum decays more rapidly, yielding a slope of roughly -3, that has been observed during several investigations of highly buoyant flows with molecular Prandtl/Schmidt numbers in the range 0.7–7, but not in nonbuoyant flows (Mizushima et al, 1979; Papanicolaou and List, 1987, 1988). Papanicolaou and List (1987) argue that this portion of the spectrum agrees with the behavior expected for the inertial-diffusive subrange, where the variation of the local rate of dissipation of mixture fraction fluctuations in buoyant flows is due to buoyancy-generated inertial forces rather than viscous forces. An effect of this type is plausible due to the progressive increase of the span of the inertial range as $(x-x_o)/d$ increases, e.g., the intersections of the $-5/3$ and -3 regions of the spectra occur at roughly $n\tau_f = 0.4$, 0.8, 1.5, and 2.0 for $(x-x_o)/d = 25$, 50, 99, and 151, respectively. This behavior is analogous to the anticipated reductions of microscales with increasing streamwise distance, which suggests a diffusive effect. However, understanding of the behavior of the spectra of buoyant turbulent flows in this region is very limited and clearly merits additional study. At higher frequencies, the mixture fraction microscale should be approached where the spectrum becomes small; unfortunately, existing measurements have had neither the spatial nor the temporal resolution needed to resolve this region.

Radial Spatial Correlations. Spatial correlations also must be known in order to simulate aspects of radiation fluctuations, due to effects of optical path lengths on radiation intensities (Kounalakis et al., 1991). Spatial correlations also are important fundamental properties of turbulence that have received significant attention in the past (Hinze, 1975; Tennekes and Lumley, 1972). Study of these properties was begun during the present investigation by measuring radial spatial correlations, which largely control radiation fluctuations in boundary layer flows, like plumes (Kounalakis et al., 1991).

The general properties of spatial correlations in turbulent shear flows vary depending on whether the two points considered are on the same or on opposites sides of planes or lines of symmetry. This orientation will be indicated for the present radial correlations by a coordinate system along the radial direction extending from $-\infty$ to ∞ with Δr always greater than zero and the left-most position denoting the position of the correlation. Thus, $r<0$ implies that both points are on the same side of the axis for $\Delta r<|r|$ and on the opposite side thereafter. If $r>0$, then both points are always on the same side of the axis. Finally, Corrsin and Uberoi (1950) introduced symmetric lateral spatial correlations for jets, where the two points are spaced equally on either side of the axis (at $-\Delta r/2$ and $\Delta r/2$), thus, there is only one correlation of this type at each streamwise position.

The present measurements of two-point radial and symmetric correlations are illustrated in Fig. 7. These results are for carbon dioxide plumes at $(x-x_o)/d = 87$, which is within the self-preserving region. Other measurements within the self-preserving region were similar. The measurements are presented in two groups, with results for $r>0$ at the top, and results for $r<0$ and symmetric correlations at the bottom. The distance increment is normalized by Λ_{frc}; however, Λ_{fr} is relatively constant over the range of the measurements. The results for $r>0$ in Fig. 7 exhibit an exponential decay; however, this is an artifact of experimental limitations, e.g., the region near $\Delta r = 0$ should have a nonexponential (quadratic) behavior in terms of Δr as the microscale limit is approached (Becker et al., 1967; Hinze, 1975; Tennekes and Lumley, 1972). This

is not seen in Fig. 7 because the present spatial resolution was not adequate to resolve the smallest scales. In terms of $\Delta r/\Lambda_{frc}$ the exponential fit of the radial spatial resolution was not adequate to resolve the smallest scales. In terms of $\Delta r/\Lambda_{frc}$ the exponential fit of the radial spatial correction is quite simple:

$$\overline{f'(r)f'(r+\Delta r)} \;/\; \overline{f'(r)}\;\overline{f'(r+\Delta r)} = \exp(-\Delta r/\Lambda_{frc}) \quad (10)$$

where it should be understood that $\Delta r > 0$ as defined earlier. The results in Fig. 7 show that Eq. (10) provides a good fit of the measurements whenever both points of the correlation are on the same side of the axis, e.g., $r > 0$ or $\Delta r < |r|$ when $r < 0$. This approximation is effective because Λ_{fr} is relatively constant over the range of the measurements, as noted earlier. Notably, a radial spatial correlation at the plume axis in the self-preserving region, reported by Papantoniou and List (1989), has essentially the same shape as Eq. (10).

The symmetric spatial correlation provides the other limiting behavior of the radial spatial correlations seen in Fig. 7. These correlations exhibit a Frenkiel function shape as follows: similar to the exponential fit at small Δr; crossing to a region of negative correlations at $\Delta r/\Lambda_{frc} = 2.1$, which corresponds to $\Delta r/(x-x_o) = 0.07$; reaching a maximum negative value of -0.1 near $\Delta r/\Lambda_{frc} = 4$, which corresponds to $\Delta r/(x-x_o) = 0.13$; and finally decaying from the negative side toward zero as $\Delta r/\Lambda_{frc}$ becomes large. This behavior can be represented by the following empirical fit:

$$\overline{f'(\Delta r/2)f'(-\Delta r/2)} \;/\; \overline{f'(\Delta r/2)^2} = (1-0.11(\Delta r/\Lambda_{frc})^3)\exp(-\Delta r/\Lambda_{frc}) \quad (11)$$

The present behavior is qualitatively similar to symmetric correlations observed in nonbuoyant jets, except that the negative correlation region is reached sooner in jets, $\Delta r/(x-x_o)$ in the range 0.04–0.06, and the maximum negative correlation is larger in jets, in the range -0.10 to -0.18 (Corrsin and Uberoi, 1950; Becker et al., 1967).

The Frenkiel function behavior of the symmetric correlation is probably caused by the requirement for conservation of scalar flux. In particular, fluctuations of one sign must be compensated by fluctuations of the other sign on opposite sides of the axis so that the mixture fraction flux is preserved as a whole. Similar behavior is well known for the lateral spatial correlations of velocity fluctuations in isotropic turbulence due to conservation of mass requirement (Hinze, 1975). The rather slow final decay of the negative portion of the symmetric correlation, in comparison to the exponential decay for $r > 0$, also tends to support a large-scale requirement of this type. Unfortunately, interpreting the Frenkiel function shape of the symmetric correlation will require information about velocities (or scalar fluxes) that currently is not available.

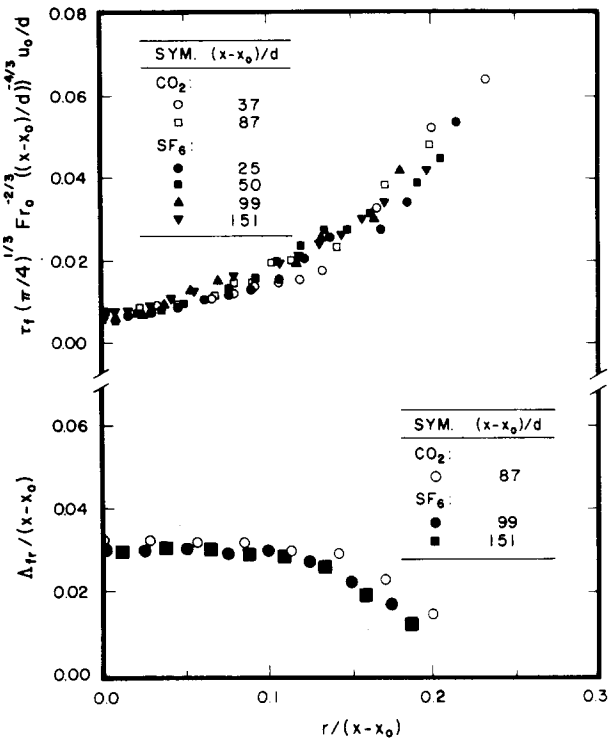

Fig. 8 Radial distributions of temporal and radial spatial integral scales

The measured spatial correlations for negative r in Fig. 7 generally are intermediate between the exponential and Frenkiel function limits. Naturally, the exponential correlation is retrieved exactly when $\Delta r < |r|$ and both points are on the same side of the axis. On the other hand, when $\Delta r \approx 2|r|$ for $r < 0$, the symmetric correlation is retrieved. Not surprisingly, other values of Δr generally represent an interpolation between these two limits. Most of the complexities of radial spatial correlations however, involve relatively small values of the correlations, which should not have a large effect on radiation fluctuations.

Integral Scales. The properties of the temporal power spectra and radial spatial correlations are completed by the corresponding temporal and spatial integral scales. Present measurements of the integral scales are plotted as a function of radial distance in Fig. 8 for both sources. The measurements extend into the self-preserving region, $25 \le (x-x_o)/d \le 151$; however, effects of streamwise distance are relatively small when plotted in the manner of Fig. 8.

The temporal integral scales at the top of Fig. 8 have been plotted by adopting Taylor's hypothesis for the relationship between spatial and temporal integral scales. Then the temporal integral scales have been normalized using self-preserving turbulent plume scaling relationships, i.e., length scales are proportional to $(x-x_o)$ and the velocity scales of the self-preserving region (Rouse et al., 1952; List, 1982). This approach seems robust and provides a good correlation of the temporal integral scales over the range of the present measurements. The results show a progressive increase of τ_f with radial distance. This follows from Taylor's hypothesis because spatial integral scales are relatively independent of radial position (see the lower part of Fig. 8) while streamwise mean velocities decrease as the edges of the plumes are approached.

The radial spatial integral scales for the plumes in the present self-preserving region, $(x-x_o)/d \ge 87$, are plotted in the lower part of Fig. 8. These integral scales were found from the correlations for positive values of r, as discussed previously. They have been normalized by $(x-x_o)$ to indicate scaling in the self-preserving region, similar to the temporal integral scales. The results indicate relatively little variation of Λ_{fr} for $r/(x-x_o) < 0.15$, followed by a reduction toward zero at large radial distances. This behavior follows from the intermittency of the flow at larger radial distances where the dimensions of turbulent fluid having mixture fractions greater than zero must decrease progressively. Present measurements yield $\Lambda_{fr}/(x-x_o) = 0.033$ near the axis $(r/(x-x_o) < 0.09)$ within the self-preserving region $((x-x_o)/d \ge 87)$. In contrast, Papantoniou and List (1989) report somewhat scattered and consistently lower values of $\Lambda_{fr}/(x-x_o)$ at comparable streamwise distances, in the range 0.011–0.022 for $r/(x-x_o) \le 0.044$. The large Schmidt numbers of the liquid plumes considered by Papantoniou and List (1989) may be responsible for the differences between the two studies because this allows larger amounts of unmixed fluid to penetrate the flow than in gaseous plumes. Thus, large Schmidt numbers would tend to reduce spatial correlations, while increasing concentration fluctutaions as discussed earlier.

Conclusions

Mixture fraction statistics were measured in round buoyant

turbulent plumes in still air. The test conditions involved buoyant jet sources of carbon dioxide and sulfur hexafluoride to give ρ_o/ρ_∞ of 1.51 and 5.06 and source Froude numbers of 7.80 and 3.75, respectively, with $(x-x_o)/d$ in the range 0–151 and $(x-x_o)/l_M$ in the range 0–43. The major conclusions are as follows:

1 The present measurements, supported by earlier findings of Papanicolaou and List (1989) for similar conditions, yielded distributions of mean mixture fractions in self-preserving plumes that were up to 30 percent narrower, with scaled values at the axis up to 30 percent larger, than other results found using buoyant jet sources in the literature, e.g., Papanicolaou and List (1987, 1988), Shabbir and George (1992), George et al. (1977), and Rouse et al. (1952), among others. Based on the observation that the earlier results were similar to behavior within the transitional plume region during the present study, it appears that the earlier results were not obtained at sufficient distances from the source to reach self-preserving conditions. In particular, self-preserving conditions were reached for $(x-x_o)/d \geq 87$ during the present measurements and those of Papantoniou and List (1989), while the earlier measurements, for comparable source Froude numbers, involved $(x-x_o)/d \leq 62$. Naturally, distances from the source to reach self-preserving conditions depend on source properties like Re_o, Fr_o, and ρ_o/ρ_∞, and may be much shorter for purely buoyant sources (Kotsovinos, 1985); quantifying these effects merits additional study.

2 Radial profiles of mixture fraction fluctuations in the self-preserving region for plumes do not exhibit reduced values near the axis similar to jets. Instead, effects of buoyancy cause mixture fraction fluctuations to be maximum at the axis with intensities of roughly 45 percent. These large intensities probably are responsible for the large radiation fluctuation levels observed in the near-overfire region of fires.

3 Probability density functions of mixture fractions can be approximated reasonably well by either clipped-Gaussian or beta functions. Unlike nonbuoyant turbulent jets, finite levels of intermittency are observed at the axis within the self-preserving region of turbulent plumes.

4 The low-frequency portion of the temporal spectra of mixture fraction fluctuations is a robust property of plumes, which scale in a relatively universal manner even in the transitional plume region. The spectra exhibit the well-known $-5/3$ power inertial decay region followed by a -3 power inertial-diffusive region. The latter region has been observed by others in buoyant flows but is not observed in nonbuoyant flows; thus, it is an interesting buoyancy/turbulence interaction that merits further study.

5 Radial spatial correlations were limited by correlations where both points were on the same side of the axis, which exhibited an exponential decay, and symmetric correlations, which approximated a Frenkiel function. This behavior probably follows from conservation of scalar flux considerations, but more measurements and study are required to understand the phenomena controlling spatial correlations. Behavior near microscales was not addressed during the present study due to the limited spatial resolution of the measurements.

6 Integral scales behaved as anticipated and provisional scaling relationships have been proposed that merit additional study. Temporal integral scales were smallest at the axis, which follows from Taylor's hypothesis noting than mean velocities are largest in this region. Radial spatial integral scales were largest at the axis, which follows from the topography of the flow, i.e., the streamwise extent of particular sections of partially mixed turbulent fluid must decrease as the intermittency increases toward the edge of the flow.

Acknowledgments

This research was supported by the United States Department of Commerce, National Institute of Standards and Technology, Grant No. 60NANB1D1175, with H. R. Baum of the Building and Fire Research Laboratory serving as Scientific Officer.

References

Abraham, G., 1960, "Jet Diffusion in Liquid of Greater Density," *ASCE J. Hyd. Div.*, Vol. 86, pp. 1–13.

Becker, H. A., Hottel, H. C., and Williams, G. C., 1967, "The Nozzle-Fluid Concentration Field of the Round, Turbulent, Free Jet," *J. Fluid Mech.*, Vol. 30, pp. 285–303.

Bilger, R. W., 1976, "Turbulent Jet Diffusion Flames," *Prog. Energy Combust. Sci.*, Vol. 1, pp. 87–109.

Bird, R. B., Stewart, W. E., and Lightfoot, E. N., 1960, *Transport Phenomena*, Wiley, New York, pp. 502–513.

Corrsin, H. Y., and Uberoi, M. S., 1950, "Further Experiments on the Flow and Heat Transfer in a Heated Turbulent Jet," NACA Rept. No. 998.

George, W. K., Jr., Alpert, R. L., and Tamanini, F., 1977, "Turbulence Measurements in an Axisymmetric Buoyant Plume," *Int. J. Heat Mass Trans.*, Vol. 20, pp. 1145–1154.

Hiller, B., and Hanson, R. K., 1990, "Properties of the Iodine Molecule Relevant to Laser-Induced Fluorescence Experiments in Gas Flows," *Expts. Fluids*, Vol. 10, pp. 1–11.

Hinze, J. O., 1975, *Turbulence*, 2nd ed, McGraw-Hill, New York, pp. 175–319.

Kotsovinos, N. E., 1985, "Temperature Measurements in a Turbulent Round Plume," *Int. J. Heat Mass Trans.*, Vol. 28, pp. 771–777.

Kounalakis, M. E., Sivathanu, Y. R., and Faeth, G. M., 1991, "Infrared Radiation Statistics of Nonluminous Turbulent Diffusion Flames," ASME JOURNAL OF HEAT TRANSFER, Vol. 113, pp. 437–445.

Lai, M.-C., and Faeth, G. M., 1987, "A Combined Laser-Doppler Anemometer/Laser-Induced Fluorescence System for Turbulent Transport Measurements," ASME JOURNAL OF HEAT TRANSFER, Vol. 109, pp. 254–256.

List, E. J., 1982, "Turbulent Jets and Plumes," *Ann. Rev. Fluid Mech.*, Vol. 14, pp. 189–212.

Lockwood, F. C., and Naguib, A. S., 1975, "The Prediction of Fluctuations in the Properties of Free, Round-Jet Turbulent Diffusion Flames," *Combust. Flame*, Vol. 24, pp. 109–124.

Mizushima, T., Ogino, F., Veda, H., and Komori, S., 1979, "Application of Laser-Doppler Velocimetry to Turbulence Measurements in Non-isothermal Flow," *Proc. Roy. Soc. London*, Vol. A366, pp. 63–79.

Morton, B. R., Taylor, G. I., and Turner, J. S., 1956, "Turbulent Gravitational Convection From Maintained and Instantaneous Sources," *Proc. Roy. Soc. London*, Vol. A234, pp. 1–23.

Mortion, B. R., 1959, "Forced Plumes," *J. Fluid Mech.*, Vol. 5, pp. 151–163.

Ogino, F., Takeuchi, H., Kudo, I., and Mizushima, T., 1980, "Heated Jet Discharged Vertically in Ambients of Uniform and Linear Temperature Profiles," *Int. J. Heat Mass Transfer*, Vol. 23, pp. 1581–1588.

Panpanicolaou, P. N., and List, E. J., 1987, "Statistical and Spectral Properties of Tracer Concentration in Round Buoyant Jets," *Int. J. Heat Mass Transfer*, Vol. 30, pp. 2059–2071.

Papanicolaou, P. N., and List, E. J., 1988, "Investigation of Round Vertical Turbulent Buoyant Jets," *J. Fluid Mech.*, Vol. 195, pp. 341–391.

Papantoniou, D., and List, E. J., 1989, "Large Scale Structure in the Far Field of Buoyant Jets," *J. Fluid Mech.*, Vol. 209, pp. 151–190.

Peterson, J., and Bayazitoglu, Y., 1992, "Measurements of Velocity and Turbulence in Vertical Axisymmetric Isothermal and Buoyant Plumes," ASME JOURNAL OF HEAT TRANSFER, Vol. 114, pp. 135–142.

Pivovarov, M. A., Zhang, H., Ramaker, D. E., Tatem, P. A., and Williams, F. W., 1992, "Similarity Solutions in Buoyancy-Controlled Diffusion Flame Modelling," *Combust. Flame*, Vol. 92, pp. 308–319.

Rouse, H., Yih, C. S., and Humphreys, H. W., 1952, "Gravitational Convection From a Boundary Source," *Tellus*, Vol. 4, pp. 201–210.

Shabbir, A., and George, W. K., 1992, "Experiments on a Round Turbulent Buoyant Plume," NASA Technical Memorandum 105955.

Sivathanu, Y. R., and Faeth, G. M., 1990, "Generalized State Relationships for Scalar Properties in Nonpremixed Hydrocarbon/Air Flames," *Combust. Flame*, Vol. 82, pp. 211–230.

Stårner, S. H., and Bilger, R. W., 1983, "Differential Diffusion Effects on Measurements in Turbulent Diffusion Flames by the Mie Scattering Technique," *Prog. Astro. and Aero.*, Vol. 88, pp. 81–104.

Tennekes, H., and Lumley, J. L., 1972, *A First Course in Turbulence*, MIT Press, Cambridge, MA.

Wu, J.-S., and Faeth, G. M., 1993, "Sphere Wakes in Still Surroundings at Intermediate Reynolds Numbers," *AIAA J.*, Vol. 31, pp. 1448–1455.

Zimin, V. D., and Frik, P. G., 1977, "Averaged Temperature Fields in Asymmetrical Turbulent Streams Over Localized Heat Sources," *Izv. Akad. Nauk. SSSR*, Mekhanika Zhidkosti Gaza, Vol. 2, pp. 199–203.